Diesel spray velocity and break-up characterization with dense spray imaging

D. Sedarsky, S. Idlahcen, K. Lounnaci, J. Blaisot, C. Rozé

Diesel spray velocity and break-up characterization with dense spray imaging

D. Sedarsky*, S. Idlahcen, K. Lounnaci, J.B. Blaisot, C. Rozé
CORIA, University of Rouen, France
david.sedarsky@coria.fr

Abstract

This work presents analysis methods for categorizing breakup morphology in a diesel spray produced by a single-hole, plain orifice diesel injector issuing into ambient atmospheric conditions. Velocity data and images which include the near-nozzle region of a diesel spray were obtained using both time-gated ballistic imaging (BI) and high-resolution ultrafast shadow imaging (USI) measurements. The USI results provide high-resolution visualization of the spray edges and resolved droplets within the depth-of-field of the collection optics, while the BI results provide a view of the spray at a modified dynamic range which mitigates interferences from refracted light and multiple-scattering noise, revealing additional spatial information. Time-correlated image-pairs obtained by both techniques were filtered and cross-correlated on a variety of scales to produce velocity profile data and identifiable structures which can be exploited to differentiate the breakup modes observed in the diesel spray. In addition, a multi-scale analysis was applied to the image data, demonstrating an approach whereby physical parameters can be derived from the image data to quantify the degree of atomization exhibited by a diesel spray.

Introduction

More than a third of the world's total primary energy supply, in excess of 4050 Mtoe, is currently derived from liquid petroleum fuels [1]. Thus, improving the efficiency and reducing the impact of liquid fuel combustion is essential for the development of effective and sustainable energy use. In the overwhelming number of applications, combustion is effected by vaporizing the volatile liquid fuel in a high-pressure spray and mixing with air to create an efficient gas-phase reaction. Despite its utility and widespread use, the fundamental aspects of this injection process are not fully understood, especially at conditions and scales relevant for compression ignition engines.

The sprays which have proven to be effective in diesel engines often exhibit large variations in structure, breakup length, cone angle, droplet size distribution, and overall morphology which cannot be directly linked to the main injection parameters (pressure, orifice geometry, fluid properties, etc). In addition, the large optical depth of the near-field and the sensitivity of the spray formation to disturbances in the flow field effectively prevent the application of conventional imaging or velocity diagnostics in many regions which are important for understanding spray formation. However, a number of emerging optical techniques have demonstrated that specialized measurements can be applied in the near-field, despite the severe attenuation and scattering noise endemic to dense spray regions. Notable diagnostics for dense spray investigations include x-ray absorption [2], optical connectivity [3], structured light planar imaging [4], ballistic imaging [5], and ultrafast shadow imaging [6]. The latter two techniques were applied in this work to obtain time-resolved images of a high-pressure diesel spray generated by a Common Rail fuel injection system.

The focus of the present work is the analysis of near-field spray images to identify and categorize diesel jet morphology and breakup characteristics. To this end, time-resolved BI and USI data sets are analyzed to derive statistical profiles of diesel spray velocity, and a multi-scale structure analysis is applied to sets of time-resolved images to in order to obtain a statistical metric which is indicative of the degree of atomization exhibited by the spray and relates directly to the physical characteristics of the time-resolved image data.

Measurements

The images used for the analyses presented in following sections were obtained by applying ballistic imaging (BI) and ultrafast shadow imaging (USI) to a spray generated by a single-hole diesel test injector, issuing into ambient air. The injector was mounted on a three-way translation stage housed in an enclosure with four windows, providing line-of-sight optical access in two directions. The measurements were carried out using a calibration liquid (ISO 4113) with properties similar to diesel fuel with carefully controlled viscosity, density, and surface tension specifications (see Table 1). The single-orifice injector with a hole diameter of 113 µm was supplied with fuel through a Common Rail accumulator, allowing adjustable injection pressures from 40 to

*Corresponding author: David.Sedarsky@coria.fr

100 MPa. Each injection event was controlled electronically by two current levels of 400 µs duration, at a repetition rate of 1 Hz, where the reference clock for the complete system was defined by the laser oscillator operating at 80 MHz. Figure 1 shows composite BI and USI images of the spray for three different time delays after start-of-injection (SOI).

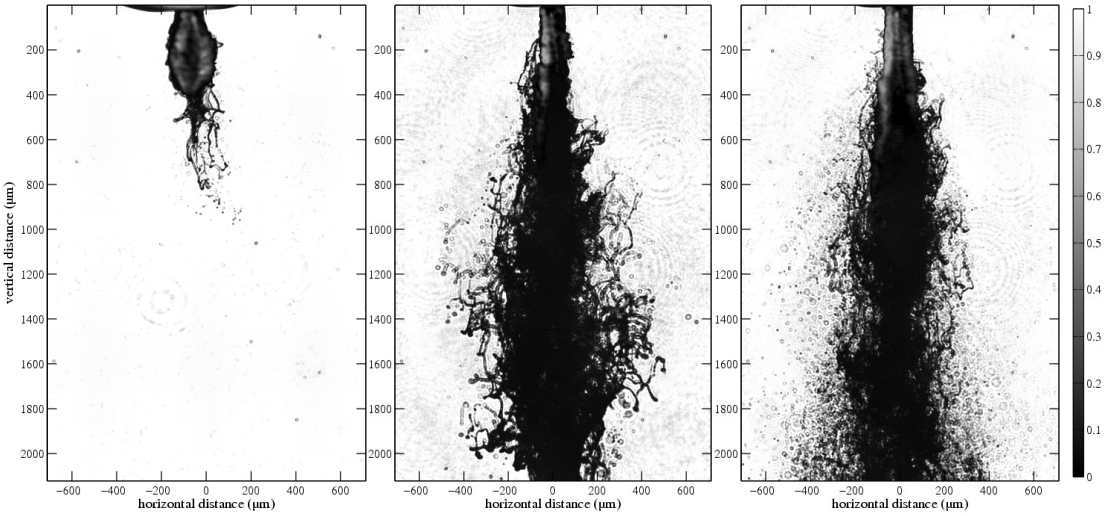

Figure 1 Diesel surrogate (ISO4113) spray images of single-hole diesel test injector, P_{inj} = 40MPa. Composite BI and USI results are shown for (a.) 5µs after SOI, (b.) 35µs after SOI, (c.) 55µs after SOI.

Ballistic imaging (BI) is a technique which selectively attenuates light transmitted through the spray to form a 2-D spatial intensity dominated by light which has been minimally distorted by scattering interactions. The primary effect of the filtering is to increase the image contrast, while decreasing overall signal intensity. The selective attenuation changes the inherent dynamic range of the detected signal, decreasing the multiply-scattered and distorted light, and increasing the relative intensity of weaker signal components. When this filtering action can be tailored to specific light properties which are changed by scattering interaction in the spray, the reduced intensity signal reveals structural information which is not present in a conventional imaging measurement, due to the dynamic range limits of the detector. Many filtering arrangements can be useful for improving image contrast, including selection based on light polarization, coherence, optical path length, and propagation direction. It is useful to think of the photons from an infinitely short plane wave crossing the medium; after they transit the spray most of these photons have interacted with one or several droplets or liquid structures [7]. Each individual scattering interaction has some probability to disturb the photon, distorting the information it represents [8]. Hence, one can view the information content of the light exiting the spray as a distribution ranging from undistorted 'ballistic' light to heavily distorted diffusely scattered light. By suppressing diffusely scattered light with low information fidelity, image contrast is improved [9].

The system used for the time-gated BI measurements included in this work is shown in Fig. 1. Source light for the system is generated by two regenerative amplifiers seeded by a single mode-locked laser oscillator. This source illuminates the spray with a pair of synchronized ultrashort (~120 fs) laser pulses at a repetition rate of 1 kHz. Light from each imaging pulse is separately used to drive two optically activated gate stages. The combined action of these gates results in an adjustable shutter which can limit light collection to an ultrashort (~200 fs) window. The imaging path is subsequently split into two detection arms by the action of a Pockels cell and a polarizing beam splitter. Each of these detection arms are equipped with a high dynamic range EM-CCD camera, allowing time-correlated ballistic images with a minimum interframe time separation of 10 ns, limited by the Pockels cell drive electronics. Post-processing and analysis of these image-pairs can subsequently yield dynamic information on the character of the spray, based on the apparent motion of the spatial intensity between corresponding images.

Table 1: Properties of ISO 4113 calibration oil.

Density	Viscosity	Surface Tension
821 kg/m^3	0.0032 kg/(m·s)	0.02547 N/m

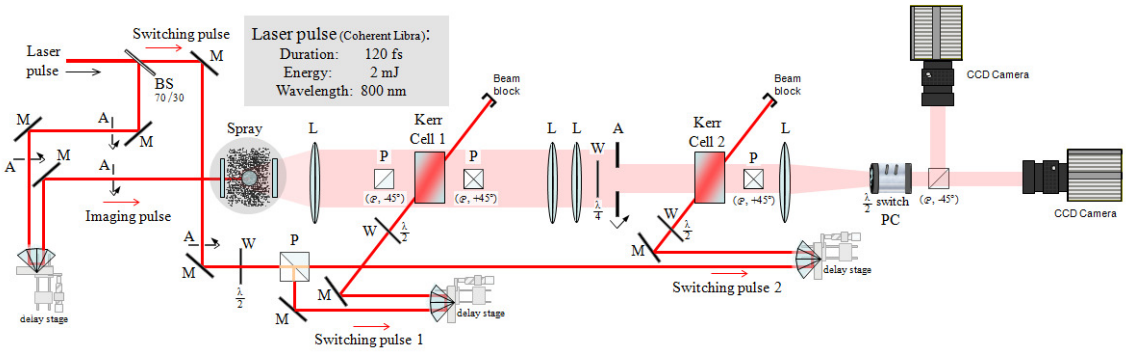

Figure 2 Double-pulse compound OKE time-gating BI system. A pair of ultrafast laser pulses are used to illuminate the spray; energy from each image pulse is divided to drive two Kerr cells, which introduce a time-dependent birefringence when active. The action of the Kerr cells together with the polarization optics, define a ~200 fs optically driven shutter which time-gates the image pulse as it transits the collection optics. The pair of image pulses from the dual-pulse laser source are directed along separate paths by the action of Pockels cell to two EM-CCD cameras to form a time-correlated image pair.

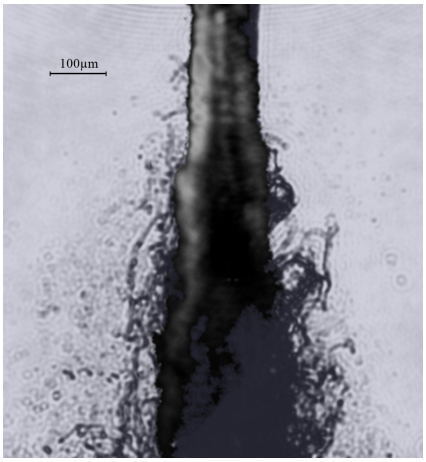

Figure 3 Ballistic image of single-hole diesel test injector (P_{inj} = 40MPa, ISO4113 calibration oil), with ~200 fs time-gating, adjusted to view refracted light inside the spray.

Light selection in this BI system is based on the filtering action of the optical Kerr cells; their combined action defines a ~200 fs time-gate which selects light based on its optical path length. Since light which scatters from droplets within the spray is dispersed according to the phase function of the scattering interaction, on average, light which is strongly disturbed will experience a longer path length than light which interacts weakly or transits the spray undisturbed (so-called 'ballistic light'). In addition, light which crosses a liquid volume within the spray will experience a longer path length due to the refractive index of the liquid fuel. This results in a temporal spreading of the optical energy which contains the information regarding the structure of the fuel spray. By selecting the first light to arrive at the detector, one can image high-contrast edge features. By tuning the time selection to account for the refractive index of the fuel, it is possible to view refracted light which transits the spray together with a selection of light delayed by scattering interactions. Figure 3 shows such an image, with the time-gate adjusted to view quasi-ballistic light at the spray center together with scattered light near the edges of the spray. Here, the vertical central line near the inlet (top) represents refracted light focused by the cylindrical geometry of the spray, and is only visible in regions where the spray surface is sufficiently uniform. The asymmetric intensity present on the left side of the image indicates that scattering interactions are occurring, increasing the path length of light near this region of the spray, allowing light into the delayed time-gate window. These disturbances are also apparent in the velocity results, which show higher velocities on this side of the spray, especially at later injection times.

Ultrafast shadow imaging (USI) is a modified shadowgraphy arrangement, which takes advantage of intense ultrashort laser illumination and the efficiency of a set of collection optics to create a 'shadow image' which is spatially resolved along the optical axis within the object plane.

In general, the 2-D spatial intensity measured by a shadowgraph system, where a light pulse illuminates a medium and light is collected in a forward-scatter geometry, results in a line-of-sight integrated projection of the source. The collected information consists of the shadow cast by all objects within the line of sight, and is commonly known as a 'shadowgram.' This type of projected shadow can contain much useful information, but it differs from a true image in a few important aspects. The phase information at the detection plane is not well-ordered and cannot be interpreted or manipulated exactly in the manner appropriate for true images, and the information possesses no appreciable spatial resolution along the optical axis. These differences are important for the application discussed here, which relies on correlation matching and analysis of spatially-resolved image features.

By utilizing an intense collimated light source to illuminate the spray and supplementing the direct shadowgraphy arrangement with light collection optics, edge features of the diesel spray which fall within the depth-of-field (DoF) of the imaging system can be resolved and separated from unfocused image regions. These data represent optical information which is spatially resolved along the optical axis of the measurement which can be used to observe and track the velocity and morphology of select structures within the spray volume [6].

Figure 4a shows the focused shadow imaging arrangement of the USI measurement. Here, collimated light from the ultrafast laser source illuminates the spray. A set of collection optics direct a focused image from the object plane to the image plane at the detector. Figure 4b highlights focused and unfocused liquid structures from a diesel spray image acquired by the USI system.

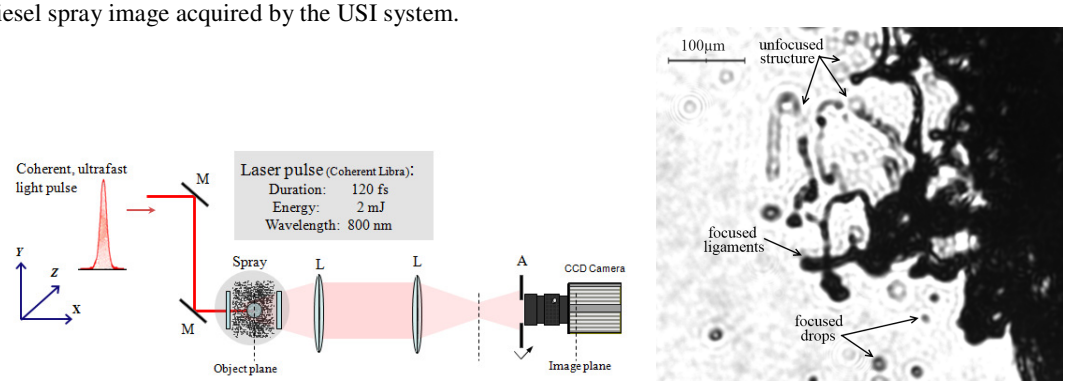

Figure 4 (a.) Ultrafast shadow imaging system. Collimated light is directed to the spray. Imaging lenses, L, are positioned to collect light from the object plane at the center of the spray to the image plane at the detector. Here the object and image planes are conjugate imaging planes of the lens system. (b.) USI measurement result, showing features on the periphery of a diesel spray, P_{inj} = 40MPa.

Velocity Analysis

A primary aim of the work presented here is to measure the velocities of liquid structures of a diesel fuel injection spray by comparing time-correlated BI and USI measurements. For the velocity information to be meaningful, the matched structure in each image-pair must be spatially resolved such that the intensity change in the images can be related to the real-world motion of the observed structure. For the measurements discussed here, this is accomplished by properly arranging the light collection optics to form focused images of structures within the spray. This, together with the quasi-cylindrical geometry of the spray formed by a single-hole injector allows the acquisition of spatially resolved image data which is amenable to analysis for dynamic information.

A variety of methods can be applied to calculate the motion of resolved structure, and hence velocity, from successive images. Velocity results presented here are based on region-matching methods which employ the normalized image cross-correlation given by

$$\frac{1}{n-1}\sum_{y,z}\frac{1}{\sigma_I\sigma_T}\left(I(y,z)-\bar{I}\right)\cdot\left(T(y,z)-\bar{T}\right) \qquad (1)$$

Here, 'search field' and 'template' image sub-regions, I(y,z) and T(y,z), are chosen from images produced by consecutive laser pulses which are spaced appropriately in time to produce time-correlated image data.In ad-

dition to the resolved features of droplets and liquid structure, the images acquired by the measurements contain unfocused regions which are not reliable for correlation analysis. These unfocused features must be suppressed or segregated from the focused structure in the images. This is accomplished in two stages, both of which identify high frequency information content in spatial intensity allowing focused image regions to contribute to the region-matching analysis and discriminating against regions with poor focus.

Prior to analysis, the images are normalized to the measured image background. The image from the first pulse is taken at time t_1; the second pulse produces an image at time, $t_2 = t_1 + \Delta t$, where Δt is given by the time delay between each pair of laser pulses. A set of rectangular image regions are selected from the t_1 image, and cross-correlated with a set of rectangular regions selected from the t_2 image, to yield the *dy/dt* and *dz/dt* components representing velocity of resolved features confined to the object plane.

The selection of appropriately located t_1 image region windows is done first by applying a Sobel edge detection scheme to the intensity data, identifying candidate regions which should be allowed to contribute to the dynamic analysis. Pixels selected by the detection scheme are randomly sampled to form template and search field image sub-regions which are processed to obtain correlation matchings.

In the second stage, the matching results and their associated image sub-regions are validated by a set of criteria which examine the spatial variance and texture energy of the image regions, and the correlation strength and bounds constraints of the matching results. With the exception of the bounds constraints, each of these validation criteria amount to a test of spatial information content for the tested region, with an associated threshold level which further discriminates image regions selected to participate in the analysis.

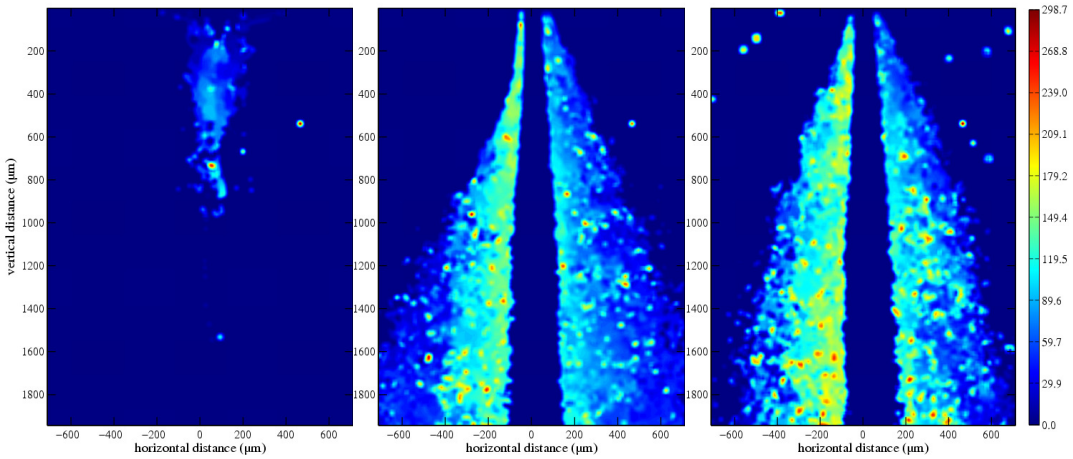

Figure 5 Statistical velocity profile map for sets of diesel surrogate (ISO4113) spray images, P_{inj} = 40MPa. Results are shown for (a.) 5µs after SOI, (b.) 35µs after SOI, (c.) 55µs after SOI. Individual images at these conditions are shown in Fig. 1.

The object-plane velocity vectors calculated for each image-pair are useful for interpreting visible spray structure in the images, and tracking their motion in two dimensions. However, due to the shot-to-shot variability of the spray it is hard to draw conclusions from individual time-resolved images. However, it is possible to compile statistical velocity profiles by combining velocity results from many time-resolved images, averaging and mapping the velocity magnitudes across the spatial extent covered by the images. Figure 5 shows velocity profiles for the image sets shown in Fig. 1, compiled using 20 x 20 pixel bins. From these images, it is clear that the spray exhibits a substantially asymmetric velocity profile which begins to develop 15 to 20 µs after SOI.

Multi-scale Analysis Method

The second aim of the work presented here is to derive a metric with a physical basis, which can be used to examine diesel spray morphology and quantify the breakup behavior exhibited by spray. Multi-scale analysis is an approach which borrows from the shape-based fractal descriptions which have proven to be effective in other chaotic systems. Efforts to apply fractal descriptions to atomizing sprays have shown that in most cases the self-similarity of turbulent sprays is limited, requiring a varying, scale-dependent, fractal dimension for complete description [10].

A surface-based scale classification scheme has been applied with some success to quasi- two-dimensional atomizing sprays. A detailed definition of the surface-based scale distribution is given in Dumouchel et al. [11]. An exceedingly brief outline of the concept is shown below.

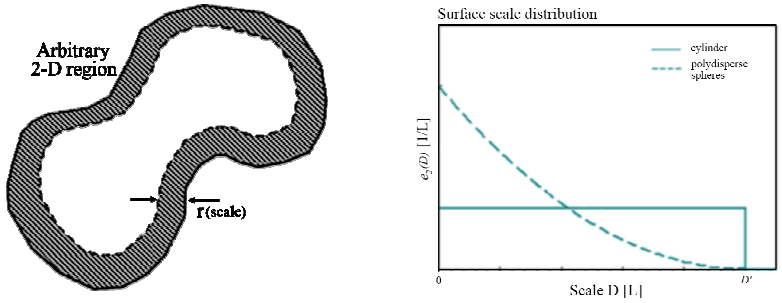

Figure 6 (a.) Illustration of a closed 2-D region of arbitrary shape and total surface area, S_T. (b.) Surface-based scale distributions for a cylinder and for a set of polydisperse

Given a closed 2-D region of arbitrary shape, as illustrated in Fig. 6a, with a total surface area, S_T. The cumulative surface-based scale distribution, $e_2(D)$ is taken to be the ratio between the surface at scale $D = 2r$ and the total surface area, S_T. The scale, D, is the distance from the shape boundary to any interior point, as such, it is allowed to vary from zero to the extent that it spans the entire shape, D'. Constraining $e_2(D \geq D') = 1$, ensures that the cumulative surface-based scale distribution lies on the interval $\{0,1\}$. For a group of N arbitrary objects, one can define the cumulative surface-based scale of the group as:

$$E_2(D) = \frac{\sum_{i=1}^{N} S_i(D)}{\sum_{i=1}^{N} S_{Ti}} \tag{2}$$

where $S_i(D)$ is the surface of object i covering the scale D and S_{Ti} is the total surface area. The distribution $e_2(D)$ is taken as the first derivative of the cumulative scale relative to D:

$$e_2(D) = \frac{dE_2(D)}{dD} \tag{3}$$

Hence, the surface-based scale distribution depends on both the size and form of the bounded region, as opposed to a basic diameter distribution which depends only on the size of the region. Figure 6b shows the distributions for a cylinder and for a set of polydisperse spheres. To a first approximation, the diesel injector spray can be viewed as a cylindrical flow which is rapidly deformed as it moves downstream and is eventually dispersed into elements dominated by surface tension—spheres characterized by some drop size distribution. Thus, one would expect the surfaced-based scale distribution describing the spray to lie somewhere between these extremes and progress from cylindrical to an ensemble of spheres result, according to the extent of atomization.

Multi-scale Results

Localized measurements of the surface-based scale distribution were carried out from the nozzle to the extent of the diesel spray image data. This local statistics analysis presents the opportunity to contrast spray morphology as the liquid mass moves downstream from the inlet. A description of the local analysis setup is shown in Fig. 7, which illustrates horizontal sections separated during the analysis.

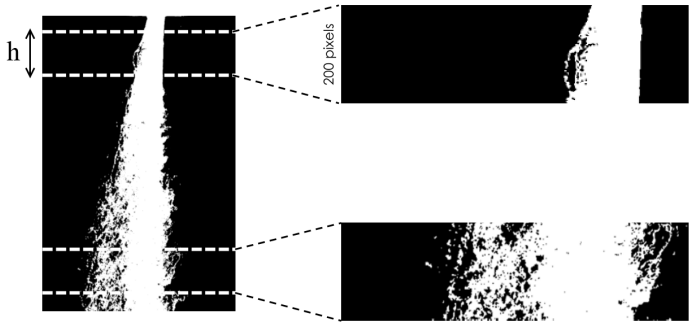

Figure 7 Horizontal sections separated for comparison of localized measurements of the surface-based scale distribution detailed in Fig. 8.

Here, a region window with a height of 200 pixels and full image width is translated over the image to calculate the distribution for each spatial step. A plot of these results are shown in Fig. 8.

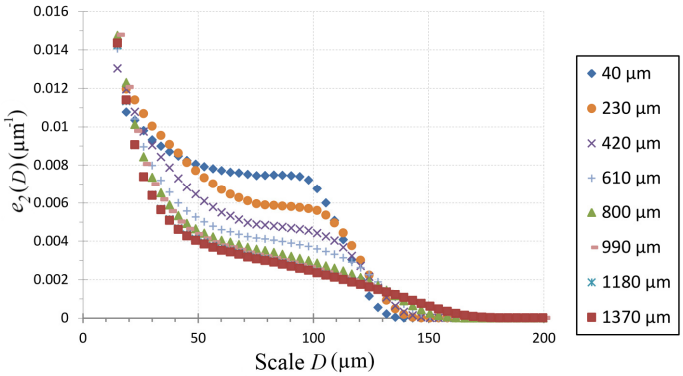

Figure 8 Evolution of the localized surface-based scale distribution versus distance from the nozzle.

Examining individual time-resolved diesel spray images, it is apparent that the spray can fluctuate to a considerable degree, and exhibits strong asymmetries under certain conditions. These deviations are of interest, since they may indicate undesirable spray behavior, or unanticipated spray morphology. In order to view and contrast the asymmetric features of the spray, the local statistics windowing approach was repeated in two separate conditions: condition 1 divides the left and right sides of the spray along the center axis of the nozzle, condition 2 divides the left and right sides by bisecting the angular spread of the spray. Figure 9 illustrates these division conditions. Results for the scale distribution versus distance from the nozzle are shown in Fig. 10 for the left and right sides using each division method.

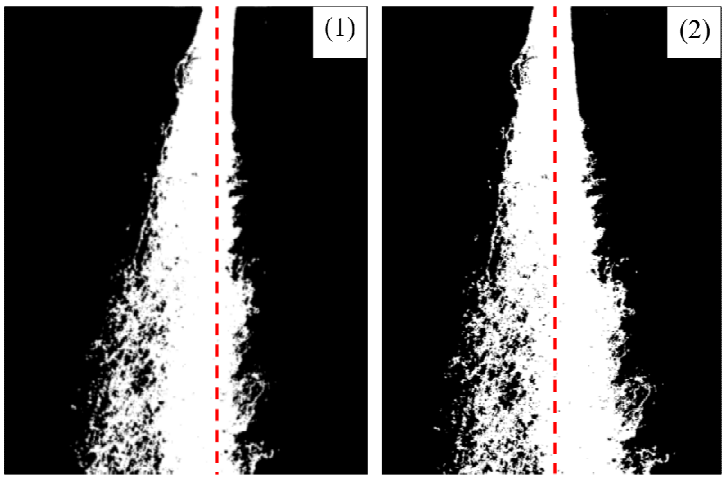

Figure 9 Vertical sections; Method (1) divides left(a) and right(b) sides of the spray along central axis defined by the nozzle, Method (2) divides the spray by bisecting the angle formed by the left and right halves of the spray.

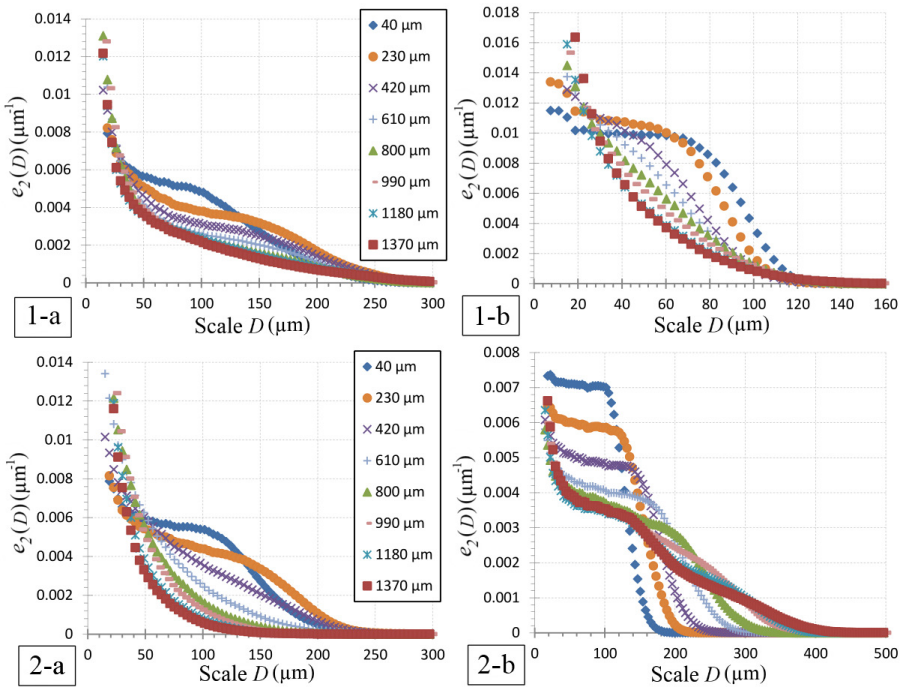

Figure 10 Evolution of the localized surface-based scale distribution versus distance from the nozzle for left (a) and right(b) sides of the spray, divided according to centerline division (1), or equal angles division (2).

Summary and Conclusions

Time-resolved image data from BI and USI measurements were used to examine spray formation in a single-hole, plain orifice test injector issuing into ambient atmospheric conditions. Time-correlated image-pairs generated by the measurements were filtered and cross-correlated to obtain velocity profile data. Results from this analysis reveal asymmetrical spray behavior, especially in the developed spray late in the injection cycle.

Multi-scale analysis was applied to the image data. Results from the multi-scale calculations confirm the asymmetries apparent in the velocity analysis and show that the surface-based scale distribution is indicative of the state of diesel spray atomization. However, calculation of the scale distribution from local statistics includes a large degree of variability depending on how the localized regions are determined.

References

[1] International Energy Agency, Paris. *Key world energy statistics*, (2011). http://goo.gl/XbwlD
[2] A. Ramírez, S. Som, Suresh Aggarwal, A. Kastengren, E. El-Hannouny, D. Longman and C. Powell, *Experiments in Fluids* 47: 119-134 (2009).
[3] Charalampous, G., Hadjiyiannis, C., Hardalupas, Y., Taylor, A., *Proceedings of ILASS Europe,* Brno, Czech Republic, No. 152 (2010).
[4] E. Kristensson, M. Richter, and M. Aldén, *Atomization and Sprays,* 20(4): 337-343, (2010).
[5] D. Sedarsky, M. Paciaroni, E. Berrocal, P. Petersson, J. Zelina, J. Gord and M. Linne, *Experiments in Fluids* 49(2): 391-408 (2010).
[6] Sedarsky, D., Idlahcen, S., Blaisot, J-B., Rozé, C., *International Symposium on Multiphase Flow and Transport Phenomena*, Agadir, Morocco, (2012).
[7] E. Berrocal, D. Sedarsky, M. Paciaroni, I. Meglinski and M. Linne, *Optics Express* 15(17): 10649-10665 (2007).
[8] E. Berrocal, D. Sedarsky, M. Paciaroni, I. Meglinski and M. Linne, *Optics Express* 17(16): 13792-13809 (2009).
[9] D. Sedarsky, E. Berrocal, and M. Linne, *Optics Express* 19(3): 1866-1883 (2011).
[10] C. Dumouchel and S. Grout, *Physica A: Statistical Mechanics and its Applications*, 390(10): 1811-1825 (2011).
[11] Dumouchel, C., Cousin, J. and Gourt, S., Journal of Flow Visualization and Image Processing, 15:59-83 (2008).
[12] E. Delacourt, B. Desmet and B. Besson, *Fuel* 84(7–8): 859-867, (2005).